JACS
JOURNAL OF THE AMERICAN CHEMICAL SOCIETY

COMMUNICATION

pubs.acs.org/JACS

Au−ZnO Hybrid Nanopyramids and Their Photocatalytic Properties

Peng Li, Zhe Wei, Tong Wu, Qing Peng, and Yadong Li*

State Key Laboratory of New Ceramics and Fine Processing, Department of Chemistry, Tsinghua University, Beijing 100084, P. R. China

Supporting Information

ABSTRACT: We successfully synthesized Au−ZnO hybrid nanoparticles with a novel hexagonal pyramid-like structure. The growth process of the as-prepared hybrid nanopyramids is clearly discussed. Because of their homogeneous composition and controlled morphology, the Au−ZnO hybrid nanopyramids demonstrate better photocatalytic efficiency than pure ZnO nanocrystals.

Colloidal hybrid nanostructures have attracted particular attention because of their unique shape- and composition-dependent properties.[1−3] Multicomponent hybrid nanomaterials with tunable composition and morphology often exhibit multiple functionalities and even novel properties, thus achieving potential applications in diverse areas such as multimodal biological detection, catalysis, solar energy conversion, and optoelectronic applications.[4,5] In recent years, significant advances in the controlled synthesis of hybrid nanocrystals (NCs) have been made.[6−8] Sun and co-workers[9] have reported a general method for producing noble-metal magnetic heterostructures based on thermal decomposition of metal carbonyls. More recently, shape-controlled binary heterostructures have been explored using faceted nanocrystals as seeds.[10] In particular, as a class of important hybrid nanomaterials, Au−semiconductor hybrid nanoparticles have become an active frontier because of their remarkable optical, electrical, and catalytic properties.[11,12] Among these hybrid nanomaterials, Au−ZnO nanocomposites with unique physical and chemical properities have been applied to dye-sensitized solar cells, photocatalysis, and biological detection.[13,15b] However, in comparison with other semiconductors, the synthesis of Au−ZnO hybrid nanostructures has achieved limited success. Therefore, there is still a lot of potential to explore facile and rational synthetic strategies for obtaining Au−ZnO hybrid NCs. In addition, hybrid NCs with homogeneous composition and controlled morphology may potentially offer enhanced photocatalytic properties.

In this work, we successfully prepared Au−ZnO hybrid nanoparticles with a novel hexagonal pyramid-like structure. The as-prepared hybrid nanopyramids (NPs) possess uniform size and morphology and interesting optical properties. The controlled synthesis of Au−ZnO hybrid NPs was based on a seed-mediated growth process. Briefly, monodisperse Au NCs (∼60 mg in 10 mL of hexane) to serve as seeds were added under agitation to a mixture of zinc acetate dihydrate (0.5 mmol), oleylamine (OAm, 3 mL), and dodecanol (DDL, 6 mL). Next, the temperature was slowly raised to 120 °C to remove water and hexane. After that, the above solution was further heated to 180 °C and kept at this temperature for a few minutes. The as-obtained products were washed with ethanol and dispersed in hexane. It is noteworthy that the hybrid materials were prepared using the common inorganic salt zinc acetate dihydrate as the metal precursor and that the reaction was conducted under mild experimental conditions without inert gas protection. Figure 1 shows a representative transmission electron microscopy (TEM) image of the Au−ZnO hybrid NPs obtained using Au NCs[14] (∼5.6 nm; see Figure S1 in the Supporting Information) as seeds. It can be seen that the nanopyramids possess a narrow size distribution and consist of a pure Au nanoparticle as the tip and a hexagonal ZnO nanopyramid as the tail (see Figure S2).

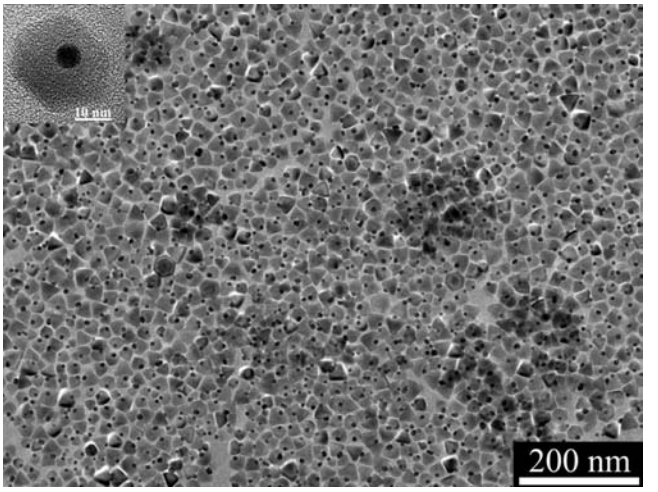

Figure 1. TEM image of the Au−ZnO nanopyramids. The inset shows a single Au−ZnO nanoparticle.

The TEM images display the ZnO nanopyramids with a side-edge length of ∼25 nm and the gold nanoparticles with an average diameter of ∼8 nm. The Au−ZnO hybrid NPs were also characterized by powder X-ray diffraction (XRD). It was found that the products are composed of wurtzite hexagonal-structured ZnO (JCPDS no. 36-1451) and cubic-phase Au (JCPDS no. 04-0784) (see Figure S4a). As shown in Figure S3, high-resolution TEM (HRTEM) images reveal that the lattice fringes correspond to the (111) and (200) planes of Au NCs and the (110), (100), and (101) planes of ZnO NCs. The high-angle annular dark-field scanning TEM (HAADF-STEM) image (Figure 2a) clearly shows the as-obtained hybrid NPs (the brighter contrast demonstrates Au). The energy-dispersive spectroscopy (EDS) mapping results (Figure 2b−e) further confirm the composition of an individual

Received: December 9, 2010
Published: March 29, 2011

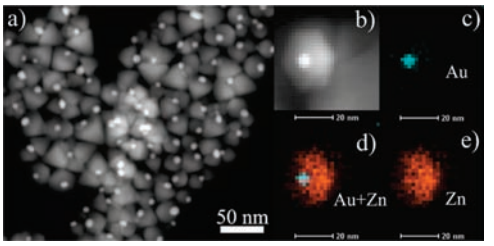

Figure 2. (a) HAADF-STEM image and (b–e) EDS maps of the as-prepared Au–ZnO nanopyramids.

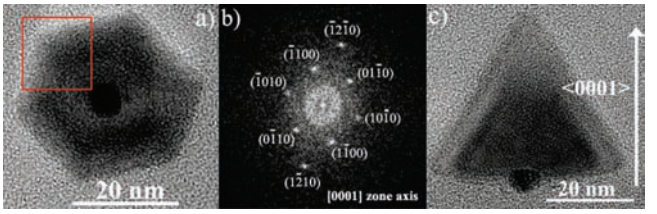

Figure 3. (a) HRTEM image of a single Au–ZnO nanoparticle. (b) FFT pattern of the selected area shown by the red square in (a). (c) TEM image of an individual particle.

hybrid nanoparticle with a head of Au and a tail of ZnO. Figure S4b shows the UV–vis absorption spectra of Au and Au–ZnO hybrid NPs. The as-prepared Au seeds exhibit strong plasmon absorption at 518 nm. It is noteworthy that in comparison with pure Au NCs, the characteristic gold plasmon peak of the Au–ZnO hybrid NPs is apparently red-shifted and broadened; this results from the size and structure of Au–ZnO hybrid NPs and the interface communication between Au and the metal oxide.[9] The absorption peak around λ = 361 nm for the Au–ZnO hybrid NPs is assigned to the ground excitonic state of pure ZnO. Moreover, the room-temperature photoluminescence (PL) was also investigated (Figure S4b inset). The Au–ZnO hybrid NPs show UV emission around λ = 393 nm, which is related to the band-edge emission of ZnO due to the recombination of excitons.

To validate the feasibility of this strategy, presynthesized Au NCs with an average diameter of ~3 nm were employed for the synthesis. Figure S5 suggests that Au–ZnO NPs were also obtained in this case. Figure 3a presents an HRTEM image of an individual Au–ZnO hybrid particle viewed along the hexagonal basal plane. Interestingly, it can be observed that the gold NC is located on the center of the basal surface, which shows that the Au seeds may selectively anchor onto the hexagonal basal surface of the ZnO NP. The corresponding fast Fourier transform (FFT) pattern (Figure 3b) demonstrates that the basal plane of the ZnO NP is perpendicular to the [0001] direction, the *c* axis of the wurtzite hexagonal structure.

In order to further investigate the growth process, aliquots of the reaction solution at different stages were withdrawn for characterization (using the ~3 nm Au seeds as an example). Figure 4 presents UV–vis spectra and typical TEM images of the products at different reaction temperatures. Interestingly, when the temperature in the system was raised to 120 °C, the maximum absorption was red-shifted to ~519 nm (see Figure S6) relative to that of the Au seeds (λ = 500 nm). The corresponding TEM image (Figure 4b) indicates that only Au NCs with an average diameter of ~6 nm are produced. Hence, the red shift of the absorption peak shows the increasing size of the Au NCs via

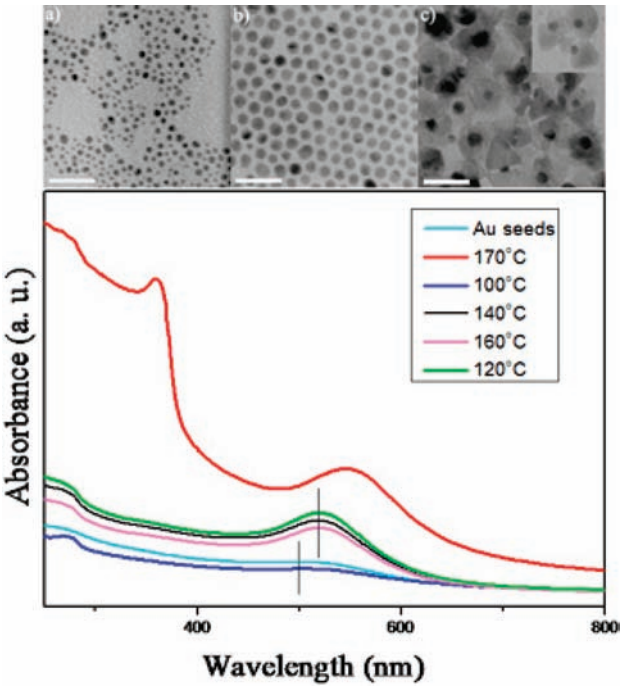

Figure 4. (a–c) TEM images (scale bars: 20 nm) and (bottom) UV–vis spectra during the growth process (the products were redispersed in hexane and then washed with ethanol).

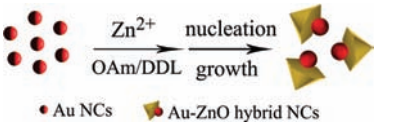

Figure 5. Schematic illustration of the formation of the Au–ZnO hybrid NPs.

Ostwald ripening during the process. After that, when the system was further heated to 170 °C, the UV–vis spectrum presents two absorption bands. To our knowledge, the absorption peak around λ = 360 nm is attributed to the ground excitonic state of pure ZnO, which may imply the presence of Au–ZnO hybrid NPs. As expected, the TEM image of the products is also consistent with the results. Herein, the monomer concentration of Zn^{2+} was low. When a high concentration of OAm was added, the nucleation occurred quickly over the presynthesized Au seeds at high temperature, and the ZnO NCs were capped by ligands of OAm less selectively. Thus, the growth along the ⟨0001⟩ direction would be reduced, resulting in the formation of ZnO with a hexagonal pyramid-like structure. Figure 4c displays the as-obtained Au–ZnO hybrid NPs with an average size of ~15 nm (side-edge length) at 170 °C. After nucleation of ZnO on the presynthesized Au seeds, the final particles with larger size can be produced with the elevated temperature.

From the above experiment results, a possible mechanism can be deduced. As described in Figure 5, when OAm and DDL were employed as solvents and capping agents, the ZnO NPs epitaxially grew over the presynthesized Au seeds. Thus, the pyramid-shaped Au–ZnO hybrid nanoparticles were formed with the Au seeds located at the basal surface. To our knowledge, the energy barrier plays an important part in the synthesis of hybrid NCs. Herein, the lower energy barrier favors the heterogeneous

dx.doi.org/10.1021/ja111102u |*J. Am. Chem. Soc.* 2011, 133, 5660–5663

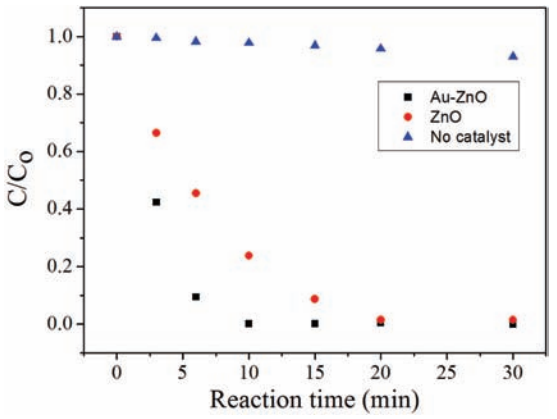

Figure 6. Photocatalytic performance of rhodamine B under UV irradiation.

nucleation of the ZnO NCs onto the Au seeds.[6b] The hexagonal basal surface of the ZnO NPs is the {0001} polar plane.[16] Because of the lower interface energy for the polar/metal interface,[8c] the Au NCs were preferentially decorated at the basal surface of ZnO. Meanwhile, possible surface defects may also exist in this region. On the other hand, the relatively large lattice mismatch (~5%), which is the lowest mismatch between {101} facets of ZnO and {111} facets of Au (Figure S3), leads to the formation of the hybrid nanostructures rather than core—shell particles.

Because of the homogeneous composition and controlled morphology, the hybrid NPs may potentially offer enhanced functions. In this work, the Au—ZnO hybrid NPs were used as an example to explore their photocatalytic property (see the Supporting Information for details). Figure 6 shows the photocatalytic degradation of rhodamine B (RhB) under UV irradiation. For comparison, the single-component of pure ZnO NCs was chosen for testing, which was achieved by etching Au—ZnO hybrid NPs with KI/I_2 solution.[15a] It is worth noting that the as-obtained ZnO NCs possess the same size distribution and morphology as the ZnO in the hybrid NPs (see Figure S7). As a result, the hybrid NPs indeed demonstrate better photocatalytic efficiency than pure ZnO NCs. It can be observed that RhB (~5 ppm) were completely degraded by the Au—ZnO hybrid NPs within 10 min (see Figure S8). In contrast, it took the pure ZnO NCs more than 20 min to achieve RhB degradation. The homogeneous component of gold NCs in the hybrid nanoparticles plays a vital role in the photocatalytic process. The enhanced photocatalytic efficiency may be attributed to the synergetic effect and specific charge-transfer kinetics in the as-prepared Au—ZnO hybrid NPs.[15]

In summary, we have prepared Au—ZnO hybrid nanoparticles with a hexagonal pyramid-like structure by regulating the heterogeneous nucleation and selective growth of ZnO on presynthesized Au seeds. It is notable that the hybrid materials were prepared using a common inorganic salt and that the reaction was conducted at mild temperatures. Moreover, the Au—ZnO hybrid NPs show higher photocatalytic efficiency than the individual ZnO NCs. Because of the simplicity and feasibility of the process, it is believed that this strategy will be suitable for scalable fabrication. On the other hand, because of their unique structure, the as-prepared hybrid NPs with uniform shape and composition are expected to provide new insights in various applications such as biological detection, solar cells, and photocatalysis.

■ ASSOCIATED CONTENT

Supporting Information. Experimental procedures and additional data. This material is available free of charge via the Internet at http://pubs.acs.org.

■ AUTHOR INFORMATION

Corresponding Author
ydli@mail.tsinghua.edu.cn

■ ACKNOWLEDGMENT

This work was supported by the State Key Project of Fundamental Research for Nanoscience and Nanotechnology (2011CB932401) and the Foundation for Innovative Research Groups of the National Natural Science Foundation of China (Grant 20921001).

■ REFERENCES

(1) (a) Dong, A. G.; Chen, J.; Vora, P. M.; Kikkawa, J. M.; Murray, C. B. *Nature* **2010**, *466*, 474. (b) Mokari, T.; Rothenberg, E.; Popov, I.; Costi, R.; Banin, U. *Science* **2004**, *304*, 1787. (c) Yin, Y. D.; Rioux, R. M.; Erdonmez, C. K.; Hughes, S.; Somorjai, G. A.; Alivisatos, A. P. *Science* **2004**, *304*, 711. (d) Cho, K. S.; Talapin, D. V.; Gaschler, W.; Murray, C. B. *J. Am. Chem. Soc.* **2005**, *127*, 7140. (e) Shevchenko, E. V.; Bodnarchuk, M. I.; Kovalenko, M. V.; Talapin, D. V.; Smith, R. K.; Aloni, S.; Heiss, W.; Alivisatos, A. P. *Adv. Mater.* **2008**, *20*, 4323.

(2) (a) Smith, A. M.; Nie, S. M. *Acc. Chem. Res.* **2010**, *43*, 190. (b) Peng, X. G. *Acc. Chem. Res.* **2010**, *43*, 1387.

(3) (a) Lisiecki, I.; Walls, M.; Parker, D.; Pileni, M. P. *Langmuir* **2008**, *24*, 4295. (b) Hochepied, J. F.; Pileni, M. P. *J. Appl. Phys.* **2000**, *87*, 2472.

(4) (a) Xu, C.; Xie, J.; Ho, D.; Wang, C.; Kohler, N.; Walsh, E. G.; Morgan, J. R.; Chin, Y. E.; Sun, S. H. *Angew. Chem., Int. Ed.* **2008**, *47*, 173. (b) Choi, S. H.; Na, H. B.; Park, Y. I.; An, K.; Kwon, S. G.; Jang, Y.; Park, M.-h.; Moon, J.; Son, J. S.; Song, I. C.; Moon, W. K.; Hyeon, T. *J. Am. Chem. Soc.* **2008**, *130*, 15573. (c) Choi, J. S.; Jun, Y. W.; Yeon, S. I.; Kim, H. C.; Shin, J. S.; Cheon, J. *J. Am. Chem. Soc.* **2006**, *128*, 15982. (d) Costi, R.; Saunders, A. E.; Elmalem, E.; Salant, A.; Banin, U. *Nano Lett.* **2008**, *8*, 637. (e) Wang, D. S.; Li, Y. D. *J. Am. Chem. Soc.* **2010**, *132*, 6280. (f) Yu, T.; Zeng, J.; Lim, B.; Xia, Y. N. *Adv. Mater.* **2010**, *22*, 5188.

(5) (a) Gur, I.; Fromer, N. A.; Geier, M. L.; Alivisatos, A. P. *Science* **2005**, *310*, 462. (b) Yu, Y. H.; Kamat, P. V.; Kuno, M. *Adv. Funct. Mater.* **2010**, *20*, 1464. (c) Bang, J. H.; Kamat, P. V. *ACS Nano* **2009**, *3*, 1467. (d) Malko, A. V.; Mikhailovsky, A. A.; Petruska, M. A.; Hollingsworth, J. A.; Htoon, H.; Bawendi, M. G.; Klimov, V. I. *Appl. Phys. Lett.* **2002**, *81*, 1303. (e) Kazes, M.; Lewis, D. Y.; Banin, U. *Adv. Funct. Mater.* **2004**, *14*, 957. (f) Zhang, J. T.; Tang, Y.; Lee, K.; Ouyang, M. *Nature* **2010**, *466*, 91.

(6) (a) Xie, R. G.; Peng, X. G. *Angew. Chem., Int. Ed.* **2008**, *47*, 7677. (b) Costi, R.; Saunders, A. E.; Banin, U. *Angew. Chem., Int. Ed.* **2010**, *49*, 4878. (c) Cozzoli, P. D.; Pellegrino, T.; Manna, L. *Chem. Soc. Rev.* **2006**, *35*, 1195. (d) Hao, R.; Xing, R. J.; Xu, Z. C.; Hou, Y. L.; Gao, S.; Sun, S. H. *Adv. Mater.* **2010**, *22*, 2729.

(7) Ohnuma, A.; Cho, E. C.; Camargo, P. H. C.; Au, L.; Ohtani, B.; Xia, Y. N. *J. Am. Chem. Soc.* **2009**, *131*, 1352.

(8) (a) Gu, H. W.; Zheng, R. K.; Zhang, X. X.; Xu, B. *J. Am. Chem. Soc.* **2004**, *126*, 5664. (b) Shi, W. L.; Zeng, H.; Sahoo, Y.; Ohulchanskyy, T. Y.; Ding, Y.; Wang, Z. L.; Swihart, M.; Prasad, P. N. *Nano Lett.* **2006**, *6*, 875. (c) Figuerola, A.; van Huis, M.; Zanella, M.; Genovese, A.; Marras, S.; Falqui, A.; Zandbergen, H. W.; Cingolani, R.; Manna, L. *Nano Lett.* **2010**, *10*, 3028. (d) Gu, H.; Yang, Z.; Guo, J.; Chang, C. K.; Xu, B. *J. Am. Chem. Soc.* **2005**, *127*, 34.

(9) (a) Yu, H.; Chen, M.; Rice, P. M.; Wang, S. X.; White, R. L.; Sun, S. H. *Nano Lett.* **2005**, *5*, 379. (b) Wang, C.; Daimon, H.; Sun, S. H. *Nano Lett.* **2009**, *9*, 1493.

(10) (a) Habas, S. E.; Lee, H.; Radmilovic, V.; Somorjai, G. A.; Yang, P. D. *Nat. Mater.* **2007**, *6*, 692. (b) Fan, F. R.; Ding, Y.; Liu, D. Y.; Tian, Z. Q.; Wang, Z. L. *J. Am. Chem. Soc.* **2009**, *131*, 12036.

(11) Zhang, J. T.; Tang, Y.; Lee, K.; Ouyang, M. *Science* **2010**, *327*, 1634.

(12) (a) Sun, Z. H.; Yang, Z.; Zhou, J. H.; Yeung, M. H.; Ni, W. H.; Wu, H. K.; Wang, J. F. *Angew. Chem., Int. Ed.* **2009**, *48*, 1. (b) Menagen, G.; Macdonald, J. E.; Shemesh, Y.; Popov, I.; Banin, U. *J. Am. Chem. Soc.* **2009**, *131*, 17406. (c) Lee, J. S.; Shevchenko, E. V.; Talapin, D. V. *J. Am. Chem. Soc.* **2008**, *130*, 9673. (d) Kuo, C. H.; Hua, T.; Huang, M. H. *J. Am. Chem. Soc.* **2009**, *131*, 17871. (e) Zeng, J.; Huang, J. L.; Liu, C.; Wu, C. H.; Lin, Y.; Wang, X. P.; Zhang, S. Y.; Hou, J. G.; Xia, Y. N. *Adv. Mater.* **2010**, *22*, 1936.

(13) (a) Chen, Z. H.; Tang, Y. B.; Liu, C. P.; Leung, Y. H.; Yuan, G. D.; Chen, L. M.; Wang, Y. Q.; Bello, I.; Zapien, J. A.; Zhang, W. J.; Lee, C. S.; Lee, S. T. *J. Phys. Chem. C* **2009**, *113*, 13433. (b) Wang, X.; Kong, X.; Yu, Y.; Zhang, H. *J. Phys. Chem. C* **2007**, *111*, 3836. (c) Haldar, K. K.; Sen, T.; Patra, A. *J. Phys. Chem. C* **2008**, *112*, 11650. (d) Liu, Y.; Zhong, M.; Shan, G.; Li, Y.; Huang, B.; Yang, G. *J. Phys. Chem. B* **2008**, *112*, 6484. (e) Shan, G.; Wang, S.; Fei, X.; Liu, Y.; Yang, G. *J. Phys. Chem. B* **2009**, *113*, 1468.

(14) Peng, S.; Lee, Y.; Wang, C.; Yin, H.; Dai, S.; Sun, S. H. *Nano Res.* **2008**, *1*, 229.

(15) (a) Lee, Y.; Garcia, M. A.; Huls, N. A. F.; Sun, S. H. *Angew. Chem., Int. Ed.* **2010**, *49*, 1271. (b) Subramanian, V.; Wolf, E. E.; Kamat, P. V. *J. Phys. Chem. B* **2003**, *107*, 7479. (c) Wang, C.; Yin, H. F.; Dai, S.; Sun, S. H. *Chem. Mater.* **2010**, *22*, 3277.

(16) (a) Chen, Y.; Kim, M.; Lian, G.; Johnson, M. B.; Peng, X. G. *J. Am. Chem. Soc.* **2005**, *127*, 13331. (b) Li, F.; Ding, Y.; Gao, P.; Xin, X.; Wang, Z. L. *Angew. Chem., Int. Ed.* **2004**, *43*, 5238. (c) Wang, Z. L.; Kong, X. Y.; Zuo, J. M. *Phys. Rev. Lett.* **2003**, *91*, No. 185502.